Distributed Control-Oriented Modeling of Thermoacoustic Dynamics in a Duct

Prashant G. Mehta, Marios C. Soteriou, and Andrzej Banaszuk

Abstract— In this paper, we consider the problem of control-oriented modeling of the thermoacoustic dynamics of ducted, premixed bluffbody stabilized combustion. We make a simplifying assumption of ignoring the vortex dynamics, but retain the effects of burning and fuel actuation. The thermoacoustic model arises as an interconnection of acoustics and heat-release submodels. For acoustics, we model the effects of mean reacting flow and for heat-release, we model the effects of distributed flame and fuel dynamics. We carry out a control-oriented analysis of the resulting coupled thermoacoustic model that highlights the important role of density ratio in obtaining combustion instability.

Fig. 1. Schematic of the physical problem.

I. INTRODUCTION

Flameholder stabilized premixed combustion in a duct has been a subject of extensive research in the past because it is a generic geometry of relevance to a number of power generation devices such as gas turbines and rockets. The effective operation of these devices is often plagued by **thermoacoustic instabilities** that arise due to a positive feedback coupling of the duct acoustic modes with the unsteady heat released due to combustion [1], [2]. Recent control-oriented modeling works in this area [2], [3], [4] have, for the most part, considered *simplified*, lumped representation of the combustion process and ignored fluid dynamics arising both as a consequence of exothermicity as well as vortex effects; see recent review in ref. [1]. The primary reason for ignoring the reacting fluid dynamics is the relative difficulty of modeling - in a reduced order fashion - these effects. Another feature of these earlier studies is that they typically consider the combustion region to be *compact* with respect to the acoustic wavelength - this is based upon low Mach number, small flamelength, and low acoustic frequency assumption.

In this paper, we build upon our recent work on mean flame response in [5] to obtain linear distributed acoustic and heat-release submodels that incorporate some of the reacting flow effects. We use the heat-release submodel to study the response of heat-release to distributed (acoustic) velocity perturbations. Such a response with *only* flame dynamics has been studied for lumped velocity perturbations in [6], [4], [7] and for distributed modal perturbation in the recent paper of [8]. Unlike these papers however, we incorporate the effects of exothermicity (density ratio) as
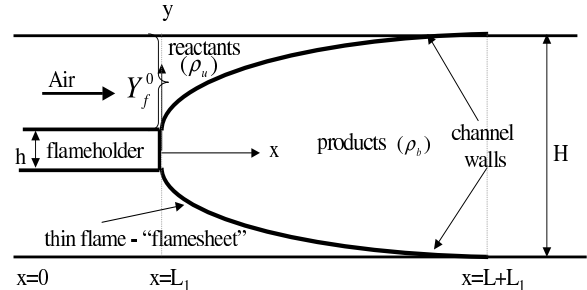
well as fuel perturbations. We also use the acoustic and heat-release submodels to carry out a control-oriented analysis of the coupled thermoacoustic problem.

The outline of this paper is as follows. In Section II, we briefly present the physical problem. In Section III, we describe the equations for distributed acoustics, and in Section IV, we build upon our work in [5] to derive a distributed model for flame/fuel dynamics and resulting heat release. In Section V, we employ the Galerkin procedure to obtain a finite-dimensional model for the coupled thermoacoustic problem and in section VI, we carry out a control-oriented analysis of this model. Finally, we draw some conclusions in Section VII.

II. PROBLEM STATEMENT

We consider the 2D physical problem of premixed combustion stabilized by a single rectangular bluff body flameholder of height h in a channel of height H (see Figure 1 for a schematic). Fuel is introduced at the trailing edge $x = L_1$, where it mixes with the incoming air to yield a uniform reactants mixture (see [9] for details on fuel injection). The Mach number is low and both reactants (of density ρ_u) and products (of density ρ_b) are assumed to behave as ideal gases. On account of the low Mach number, we assume that the density jump arises entirely because of the temperature difference between the reactants and the products. Premixed combustion is modeled using two flamesheets anchored to the two lips of the flameholder. For fluid dynamics, we retain the exothermic effects of burning but neglect vortical effects and the effect of geometrical expansion downstream of the bluffbody assuming a constant inflow of reactants with velocity U_0 (see [5], [10] for details on mean combustion models). Acoustics is introduced as perturbation to the reacting flow model and is described in the section below.

P. G. Mehta is with United Technologies Research Center East Hartford, CT 06108 mehtapg@utrc.utc.com

M. C. Soteriou is with United Technologies Research Center East Hartford, CT 06108 soterimc@utrc.utc.com

A. Banaszuk is with United Technologies Research Center East Hartford, CT 06108 banasza@utrc.utc.com

III. ACOUSTICS

The acoustics describe compressible effects of the flow that arise as perturbation of the *mean* reacting flow solution obtained with the *mean* combustion model of [5]. We start with the inviscid transport equations following the approach of [2], [9]

$$\frac{\partial \rho}{\partial t} + \nabla \cdot (\underline{u}\rho) = 0 \tag{1}$$

$$\rho\frac{\partial \underline{u}}{\partial t} + \rho\underline{u} \cdot \nabla \underline{u} = -\nabla p - \eta \tag{2}$$

$$\rho\frac{\partial e}{\partial t} + \rho\underline{u} \cdot \nabla e = -p\nabla \cdot \underline{u} + q. \tag{3}$$

In (2), η models the impact of turbulent noise. By assuming ideal gas, and substituting $e = \frac{1}{\gamma-1}\frac{p}{\rho}$ (γ denoting the ratio of specific heats) into (3) and applying (1) we obtain

$$\frac{\partial p}{\partial t} + \gamma p \nabla \cdot \underline{u} + \underline{u} \cdot \nabla p = (\gamma - 1)q. \tag{4}$$

Next, we use the decomposition

$$\begin{aligned}
\underline{u} &= \underline{U} + \hat{\underline{u}}, & p &= P + \hat{p}, \\
\rho &= \rho_0 + \hat{\rho}, & q &= Q + \hat{q},
\end{aligned} \tag{5}$$

to obtain the energy equation for acoustics

$$\begin{aligned}
\frac{\partial p}{\partial t} &+ (\underline{U} \cdot \nabla)p + \nabla P \cdot \underline{u} + \gamma P(\nabla \cdot \underline{u}) + \gamma(\nabla \cdot \underline{U})p \\
&+ \gamma p(\nabla \cdot \underline{u}) + (\underline{u} \cdot \nabla)p = (\gamma - 1)q,
\end{aligned} \tag{6}$$

where, as a matter of notation, we have dropped the hats on the perturbation variables. Denoting speed of sound $c^2 = \frac{\gamma P}{\rho_0}$, and using the continuity equation for the hydrodynamic mean $\underline{U}$, we obtain

$$\begin{aligned}
\frac{\partial p}{\partial t} &+ (\underline{U} \cdot \nabla)p + \nabla P \cdot \underline{u} + \gamma\mu S_T \delta(\underline{x} - \bar{\underline{x}}_f)p \\
&+ \rho_0 c^2(\nabla \cdot \underline{u}) + (\underline{u} \cdot \nabla)p + \gamma p(\nabla \cdot \underline{u}) = (\gamma - 1)q,
\end{aligned} \tag{7}$$

where $\bar{\underline{x}}_f$ denotes the mean flame location and the mean hydrodynamic pressure due to flow is given by

$$\nabla P = -\rho_0(\underline{U} \cdot \nabla)\underline{U}. \tag{8}$$

The momentum equation for the acoustics is given by

$$\rho_0\left[\frac{\partial \underline{u}}{\partial t} + (\underline{U} \cdot \nabla)\underline{u} + (\underline{u} \cdot \nabla)\underline{U} + \underline{u} \cdot \underline{u}\right] = -\nabla p - \eta, \tag{9}$$

where, we have neglected additional terms involving ρ on the left hand side because of the low Mach number assumption. For the purpose of this study, we write $\underline{u} = (u, v)$ and assume longitudinal acoustics with

$$v \approx 0, \quad \frac{\partial}{\partial y} = 0, \tag{10}$$

an assumption that leads to two scalar equations (describing acoustics) in two unknowns (p, u) that - after ignoring the nonlinear terms - yields

$$\begin{aligned}
\left.\begin{array}{r}
\frac{\partial p}{\partial t} + U\frac{\partial p}{\partial x} + \gamma\mu S_T\delta(\underline{x} - \bar{\underline{x}}_f)p \\
- \left[\rho_0 U\frac{\partial U}{\partial x}\right]u + \rho_0 c^2\frac{\partial u}{\partial x}
\end{array}\right\} &= (\gamma - 1)q, \\
\rho_0\frac{\partial u}{\partial t} + \rho_0\frac{\partial(Uu)}{\partial x} &= -\frac{\partial p}{\partial x} - \eta_u,
\end{aligned} \tag{11}$$

where η_u denotes the u co-ordinate of turbulent noise - we drop the subscript u subsequently. We require mean flow and flame solutions to determine the coefficients of the acoustics model (11). For this, we use the reduced order mean models derived in [5] to obtain mean axial flow

$$U(x,y) = \left\{\begin{array}{ll} U_0 & x \in [0, L_1] \\ U_0 + 2\alpha(x - L_1) & x \in [L_1, L_T] \end{array}\right., \tag{12}$$

where $\alpha = \frac{\mu S_T^0}{H}$, $\mu = (\frac{\rho_u}{\rho_b} - 1)$, and $S_T^0 = S_T[Y_f^0]$ is the flame speed (evaluated as a function of local fuel mass fraction [10]) for the uniformly premixed mean flow. The mean flame location $\bar{\underline{x}}_f = (\bar{\xi}(y), y)$ for the upper flame is obtained as the solution of G-equation [5]

$$\begin{aligned}
\left(S_T^0 + 2\alpha(\frac{H}{2} - y)\right)\frac{\partial\bar{\xi}}{\partial y} &= U_0 + 2\alpha(\bar{\xi} - L_1), \\
\bar{\xi}(x = L_1, y = \frac{h}{2}) &= 0,
\end{aligned} \tag{13}$$

whose solution (valid for $y \in [\frac{h}{2}, \frac{H}{2}]$) is given by

$$\bar{\xi}(y) = L_1 + \frac{U_0}{2\alpha}\frac{y - \frac{h}{2}}{b - y}, \tag{14}$$

where $b = \frac{H}{2}\left(1 + \frac{1}{\mu}\right)$. The solution for the lower flame is obtained as a symmetric reflection (about $y = 0$) of the upper flame solution. The length of the combustion domain over which the flame exists is obtained from the flame solution (14) by substituting $y = \frac{H}{2}$ to obtain

$$L = \frac{U_0}{S_T^0}\left[\frac{H}{2} - \frac{h}{2}\right]. \tag{15}$$

Finally, the acoustic boundary conditions are assumed to be choked-choked at the combustor inlet and exit, i.e.,

$$u(x = 0, t) = u(x = L_T, t) = 0. \tag{16}$$

IV. HEAT-RELEASE

After [5], we begin with a model for flame dynamics - written here for the upper flame - in the presence of longitudinal acoustic velocity perturbation

$$\begin{aligned}
\frac{\partial \xi}{\partial t} + (S_T + 2\alpha(\frac{H}{2} - y))\frac{\partial \xi}{\partial y} &= U_0 + 2\alpha(\xi - L_1) + u, \\
\xi(x = L_1, y = \frac{h}{2}) &= 0,
\end{aligned} \tag{17}$$

where $S_T = S_T^0 + S_T'y_f$, the second term represents the effect of fuel perturbation y_f *at* the flame - $S_T' = \frac{dS_T}{dY_f}[Y_f^0]$ is the derivative of the flame speed function evaluated at its nominal uniformly premixed fuel mass fraction Y_f^0. The

infinitesimal fuel or acoustic velocity perturbation leads to the linearized flame response (valid for $y \in [\frac{h}{2}, \frac{H}{2}]$)

$$\frac{1}{2\alpha}\frac{\partial \hat{\xi}}{\partial t} + (b - y)\frac{\partial \hat{\xi}}{\partial y} - \hat{\xi} = \frac{u}{2\alpha} - \frac{U_0}{2\alpha}\frac{S_T'}{S_T^0}y_f,$$

$$\hat{\xi}(y = \frac{h}{2}, x = L_1) = 0, \quad (18)$$

where $\xi(y,t) = \bar{\xi}(y) + \hat{\xi}(y,t)$ is the instantaneous flame location. On taking the Laplace transform of (18), making a co-ordinate change $y \to x$ [5], and multiplying the resulting equation by integrating factor, we obtain

$$\frac{d}{dx}\left[\hat{\xi}(x)a(x)^{\frac{s}{2\alpha}-1}\right] = \left[\frac{u(x)}{U_0} - \frac{S_T'}{S_T^0}y_f(x)\right]a(x)^{\frac{s}{2\alpha}-2}, \quad (19)$$

where $a(x) \doteq 1 + \frac{2\alpha}{U_0}(x - L_1)$ and explicit integration gives

$$\hat{\xi}(x) = \frac{1}{a(x)^{\frac{s}{2\alpha}-1}}\int_{L_1}^{x}a(z)^{\frac{s}{2\alpha}-2}\left[\frac{u(z)}{U_0} - \frac{S_T'}{S_T^0}y_f(z)\right]dz. \quad (20)$$

We note that here, as in remainder of this paper, identical notation is used for denoting both the variable as well as its Laplace transform. The fuel perturbation $y_f(x, t)$ at the flame arises as a consequence of the fuel perturbation

$$y_f^0 = Y_f^0 \left[-\frac{u}{U_0} + u_c\right]\Bigg|_{x=L_1} \quad (21)$$

at the fuel injection surface (see [9]) convecting to the flame location. The two perturbations may be related as

$$y_f(x, t) = y_f^0(t - \tau(x)), \quad (22)$$

by modeling the convection as a distributed delay $\tau(x) = \frac{1}{2\alpha}\log(1 + \frac{2\alpha}{U_0}(x - L_1))$ that arises because the fuel perturbation y_f^0 convects to the distributed flame with the axial reacting mean flow velocity U in (12); u_c in (21) represents the fuel control input. On combining (21) and (22) and taking the Laplace transform, we obtain

$$y_f = e^{-s\tau(x)}Y_f^0 \left[-\frac{u}{U_0} + u_c\right]\Bigg|_{x=L_1}$$

$$= a(x)^{-\frac{s}{2\alpha}}Y_f^0 \left[-\frac{u}{U_0} + u_c\right]\Bigg|_{x=L_1}. \quad (23)$$

Finally, infinitesimal flame and fuel perturbation leads to heat release perturbation

$$\frac{q}{\rho_u} = Q_F\left[\left(1 + \frac{(S_T Y_f)'}{S_T^0 Y_f^0}y_f\right)\delta(\underline{x} - \underline{x}_f) - \delta(\underline{x} - \bar{\underline{x}}_f)\right], \quad (24)$$

where $Q_F \doteq (\gamma - 1)\Delta H S_T^0 Y_f^0 = \mu c_u^2 S_T^0(1 + \phi)Y_f^0$, ϕ is the equivalence ratio, c_u is the speed of sound in the region of reactants, and $(S_T Y_f)'$ denotes the derivative (with respect to Y_f) evaluated at the nominal premixed fuel mass fraction Y_f^0.

V. THERMOACOUSTIC MODEL

In this section, we obtain control-oriented reduced order models from the distributed models described above.

A. Acoustics submodel

Assuming longitudinal acoustics (10) and substituting the mean flow (12) and flame (14) solutions in (11), we obtain the equations for the acoustic submodel

$$\left.\begin{array}{r}\frac{\partial p}{\partial t} + (U_0 + 2\alpha x)\frac{\partial p}{\partial x} + \gamma\mu S_T\delta(x - \bar{\xi}(y), y)p \\ -\rho_0 2\alpha(U_0 + 2\alpha x)u + \rho_0 c^2\frac{\partial u}{\partial x}\end{array}\right\} = (\gamma - 1)q,$$

$$\rho_0\frac{\partial u}{\partial t} + \rho_0(U_0 + 2\alpha x)\frac{\partial u}{\partial x} + \rho_0 2\alpha u = -\frac{\partial p}{\partial x} - \eta. \quad (25)$$

We now apply the Galerkin procedure to obtain a finite-dimensional representation of the pde model (25). On account of the choked-choked nature of the boundary conditions (16), we use the basis functions $G_n(x) = \sin(\frac{n\pi x}{L_T})$ to expand the velocity u and turbulent noise model η and $F_n(x) = -\cos(\frac{n\pi x}{L_T})$ to expand the variables p and q:

$$\frac{p}{\rho_u} = \sum_{n=1}^{N}p_n F_n(x), \qquad \frac{q}{\rho_u} = \sum_{n=1}^{N}q_n F_n(x), \quad (26)$$

$$u = \sum_{n=1}^{N}u_n G_n(x), \qquad \eta = \sum_{n=1}^{N}\eta_n G_n(x), \quad (27)$$

where N denotes the number of basis functions included in the finite-dimensional model.

On dividing (25) by the density of reactants ρ_u, taking the Laplace transform of resulting equations, and applying the Galerkin procedure, we obtain the transfer function models of acoustics, expressed symbolically as

$$(Is + D + C_1)\underline{p}^N + (C_2 - c_u^2\text{diag}(\frac{n\pi}{L_T}))\underline{u}^N = I\underline{q}^N \quad (28)$$

$$(B(s + 2\alpha) + C_3)\underline{u}^N = -\text{diag}(\frac{n\pi}{L_T})\underline{p}^N - I\underline{\eta}^N, \quad (29)$$

where the notation $\underline{p}^N \doteq \{p_n\}_{n=1}^{N}$, $\underline{u}^N \doteq \{u_n\}_{n=1}^{N}$, $\underline{q}^N \doteq \{q_n\}_{n=1}^{N}$, and $\underline{\eta}^N \doteq \{\eta_n\}_{n=1}^{N}$. For the Galerkin procedure, we use the 2D inner product

$$<u_1, u_2> \doteq \frac{2}{(HL_T)}\int_{\Omega}u_1\, u_2\, dxdy, \quad (30)$$

so that the effect of change in the mean density ρ_0 between reactants and products can be captured. Here $\Omega \doteq [0, L_T] \times [-\frac{H}{2}, \frac{H}{2}]$ - note either of the basis functions is orthonormal with respect to the inner product. Computation of individual terms is not entirely straightforward and we discuss some of these terms below. The matrix D corresponds to the damping effect due to (mean) burning, where its contribution - for Galerkin projection onto the mth mode - arises as

$$< F_m, \sum_{n=1}^{N}\gamma\mu S_T\delta(\underline{x} - \bar{\underline{x}}_f)p_n F_n >$$

$$= \sum_{n=1}^{N}\frac{2\gamma\mu S_T}{H(L_T)}\int_{\Omega}\delta(\underline{x} - \bar{\underline{x}}_f)p_n F_n(x)F_m(x)$$

$$\approx 2\gamma\alpha\sum_{n=1}^{N}p_n\frac{2}{L_T}\int_{L_1}^{L_T}F_n(x)F_m(x)dx, \quad (31)$$

where if $L_1 = 0$, then this term further simplifies to $2\gamma\alpha p_m$ and the matrix $D = 2\gamma\alpha I$; I denotes the size N identity matrix. The terms C_1 and C_3 capture the convective effect of exothermic mean flow and C_2 the effect of mean pressure on acoustics. Finally, the term B is quite important in capturing the increase in the natural frequency associated with burning (because of increase in the speed of the sound in the burning region). Its contribution - for Galerkin projection onto the mth mode - arises as

$$
\begin{aligned}
&< \quad G_m, \sum_{n=1}^{N}(s + 2\alpha)\frac{\rho_0}{\rho_u}u_n G_n > \\
&= \quad \sum_{n=1}^{N}\frac{2(s + 2\alpha)}{H(L_T)}\int_{\Omega}(1 - \nu\mathcal{X}_{Prod})G_n(x)G_m(x) \\
&= \quad (s + 2\alpha)\left[\delta_{mn} - \frac{2\nu}{H(L_T)}\int_{L_1}^{L_T}2\bar{\mathcal{Y}}(x)G_n G_m dx\right],
\end{aligned}
$$
(32)

where $\nu \doteq (1 - \frac{1}{1+\mu})$, $\mathcal{X}_{prod}$ is a characteristic function that is defined to take values 1 in the region of products and 0 in the region of reactants, and $\bar{\mathcal{Y}}(x)$ is the y co-ordinate of the mean flame. Substituting (29) into (28), we may eliminate the co-ordinate $\underline{u}^N$ and obtain a coupled oscillators model for the acoustics in pressure co-ordinate.

$$
\underline{p}^N = \mathbf{A_{pn}(s)}\underline{\eta}^N + \mathbf{A_{pq}(s)}\underline{q}^N.
$$
(33)

In order to obtain the forcing term on account of unsteady heat release (expressed in co-ordinate $\underline{q}^N$), we consider the formula for heat release perturbation (24).

B. Heat-release submodel

On projecting the heat release perturbation on to the mth mode, we obtain

$$
\begin{aligned}
q_m &= \quad g_1\int_{\Omega}(\delta(\underline{x} - \underline{x}_f) - \delta(\underline{x} - \bar{\underline{x}}_f))F_m \\
&+ \quad g_2\int_{\Omega}\delta(\underline{x} - \underline{x}_f)y_f F_m \\
&\approx \quad g_1\int_{L_1}^{L_T}\frac{d}{dx}(F_m\hat{\xi})dx + g_2\int_{L_1}^{L_T}y_f F_m dx, \\
&= \quad g_1(-1)^{m-1}\hat{\xi}(L_T) + g_2\int_{L_1}^{L_T}y_f F_m dx,
\end{aligned}
$$
(34)

where $g_1 = \frac{4Q_F}{HL_T}$ and $g_2 = \frac{(S_T Y_f)'}{S_T^0 Y_f^0}g_1$. The heat release response thus decomposes in to two parts: part 1) arising because of flame response, and part 2) arising because of upstream fuel perturbation as it is felt downstream at the (nominally fixed) flame. Using (23), the fuel perturbation at the flame

$$
y_f = a(x)^{-\frac{s}{2\alpha}}Y_f^0\left[-\sum_{n=1}^{N}G_n(L_1)\frac{u_n}{U_0} + u_c\right],
$$
(35)

where $G_n = \sin(\frac{n\pi x}{L_T})$, is easily obtained and gives the heat release response for part 2 - we denote the resulting transfer

function matrix from $\underline{u}^N \rightarrow \underline{q}^N$ as $\mathbf{A_{qu}^{f,2}}$. For obtaining the part 1 of the response, we use the flame solution (20) for the linearized flame dynamics

$$
\begin{aligned}
\hat{\xi}(L_T) &= \quad \sum_{n=1}^{N}a(L_T)^{1-\frac{s}{2\alpha}}\frac{u_n}{U_0}\int_{L_1}^{L_T}a(z)^{\frac{s}{2\alpha}-2}G_n(z)dz \\
&+ \quad a(L_T)^{-\frac{s}{2\alpha}}\left(\frac{S_T'}{S_T^0}\right)Y_f^0\sum_{n=1}^{N}\frac{u_n}{U_0}G_n(L_1)L,
\end{aligned}
$$
(36)

where the first term corresponds to flame response entirely due to acoustics and the second term to the flame response on account of fuel perturbation (effect on flame speed) - the corresponding transfer function matrices from $\underline{u}^N \rightarrow \underline{q}^N$ are denoted as $\mathbf{A_{qu}}$ and $\mathbf{A_{qu}^{f,1}}$ respectively. Since $a(L_T)^{-\frac{s}{2\alpha}} = exp^{-\frac{s}{2\alpha}\log(a(L_T))}$, the response $\mathbf{A_{qu}^{f,1}}$ arises as an effective delay. We note that the delay character is by no means apriori apparent as the heat-release response for this path arises due to acoustics→fuel→convection →flame dynamics→heat-release chain of effects. We show in the following section that at high frequencies, this is the portion of the heat release response that dominates and likely explains why delay models of heat release models are so popular in literature. Similar considerations apply in obtaining the transfer function matrix - denoted symbolically as $\mathbf{A_{qu_c}}$ - from the fuel input $u_c \rightarrow \underline{q}^N$, the heat release modal coefficients. We thus obtain the heat release model expressed symbolically as

$$
\underline{q}^N = \mathbf{A_{qu}}(s)\underline{u}^N + \mathbf{A_{qu}^f}(s)\underline{u}^N + \mathbf{A_{qu_c}}(s)u_c,
$$
(37)

where $\mathbf{A_{qu}^f}(s) = \mathbf{A_{qu}^{f,1}}(s) + \mathbf{A_{qu}^{f,2}}(s)$, the combined heat release response because of fuel perturbations arising due to acoustics. The individual transfer function matrix entries are obtained using (34)-(36).

C. Coupled model

Using the finite-dimensional models derived above, we construct a coupled thermoacoustic model as a feedback interconnection of (33) and (37). In this paper, we are mainly interested in stability characteristics and forced excitation of the primary thermoacoustic mode. For this purpose, the acoustic model is forced by (turbulent) noise further modeled by specifying

$$
\eta_1 = 1
$$
(38)

in (29).

Table I tabulates the numerical values of non-dimensional problem parameters for which the model was constructed. The speed of sound c_u in (28) is specified by its values in the *unburnt* reactants. The effect of increase in the speed of sound (because of temperature effect) on raising the acoustic modal frequencies is captured by the equivalent mean density change as described by term B in (29) presented in Section V-A. The control problem is to modify the coupled dynamics of the thermoacoustic loop by fuel manipulation - term involving u_c in (37).

Parameter	Value	Description
S_T^0/U_0	0.1	Flame speed
U_0/c_u	0.1	Inlet Mach number
h/H	0.25	Bluffbody width
L/H	$\frac{U_0}{2S_T^0}\left[1-\frac{h}{H}\right]$	Flame length (see (15))
L_1/L	1/3	Length of combustor inlet
μ	1-5	Heat release parameter
γ	1.4	Ratio of specific heats
$\frac{S_T'}{S_T^0}Y_f^0$	1	Gain in fuel $\rightarrow$ flame path
$\frac{(S_TY_f)'}{S_T^0 Y_f^0}Y_f^0$	1	Gain in fuel $\rightarrow$ heat release path

TABLE I

NUMERICAL RANGE OF NON-DIMENSIONAL PROBLEM PARAMETERS
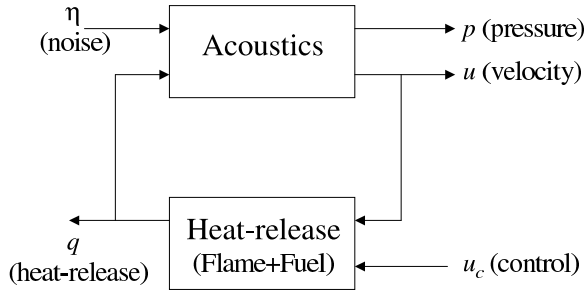
Fig. 2. Block diagram schematic of the thermoacoustic coupled model.

VI. CONTROL ORIENTED ANALYSIS

Figure 2 shows the schematic of the thermoacoustic feedback loop as an interconnection of acoustic and heat release submodels derived above. The acoustic submodel is forced by turbulent noise η^N. Figure 3 plots the frequency response from the noise input (38) to the pressure output at bluffbody trailing edge $x = L_1$ - with acoustics submodel alone - for a range of heat release parameters μ. The figure shows that as the heat-release parameter μ increases:

1) the speed of sound - in the products region - increases thereby increasing the modal frequencies, and
2) the damping of the individual modes increases because of the mean heat release effects (term D in
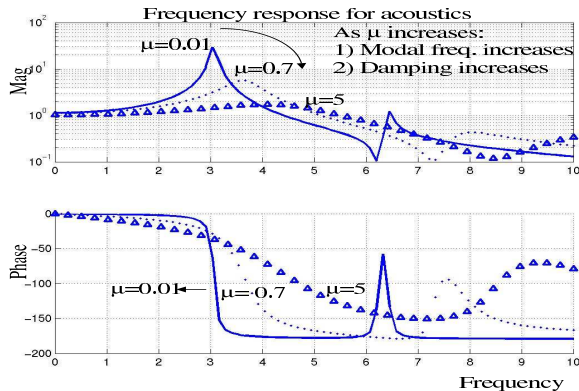

Fig. 3. Effect of density ratio on the frequency response for the acoustic submodel transfer function from noise input (38) to the pressure sensor output evaluated at $x = 0$.

(28)).

The heat release submodel is forced by the scalar control input u_c and the acoustic velocity input - modeled by $\underline{u}^N$. There are three distinct ways - captured in our model - in which acoustic perturbation causes heat release perturbation:

$\mathbf{A_{qu}}$ direct acoustic perturbation of the flame leading to perturbation in heat release,

$\mathbf{A_{qu}^{f,1}}$ acoustic perturbing the fuel and these perturbations affecting the flame motion leading to perturbation in heat release, and

$\mathbf{A_{qu}^{f,2}}$ acoustic perturbing the fuel and these perturbations directly affecting the heat release as in formulae (34).

Figure 4 compares the frequency responses due to these three effects - where we have normalized the individual responses by factor μ. As noted in Section V-B, the heat release response $\mathbf{A_{qu}^{f,1}}$ is characterized by an effective delay - the phase rolls-off while the magnitude is uniformly constant. The portion of heat release response $\mathbf{A_{qu}}$ due to the direct acoustic perturbation of flame motion arises as a low pass filter and in the limit $\mu \rightarrow 0$, yields the heat release response of [4] described in literature. Finally, the heat-release response $\mathbf{A_{qu}^{f,2}}$ due to the other fuel path - convection of fuel perturbation to a nominally fixed flame - also arises as a low pass filter. In all of these heat-release responses, as the density ratio increases, the physics of the problem becomes faster because of the acceleration due to expansion velocity and this leads to benign phase roll-off characteristics. However, the gain in the heat-release submodel also increases by a factor μ.

We finally note that the gain in the fuel dynamics path depends upon the shape of heat release nonlinearity at the mean location (normalized gains $\frac{S_T'}{S_T^0}Y_f^0$ and $\frac{S_TY_f'}{S_T^0 Y_f^0}Y_f^0$). In our analysis, we have taken these to be 1 (see Table I) although these values may be greater for lean combustion and smaller near stoichiometric limit. These values determine which of the three competing heat release responses are dominant for any frequency. However, for higher frequencies, the low pass heat release response $\mathbf{A_{qu}}$ and $\mathbf{A_{qu}^{f,2}}$ typically roll-off and the heat release response arises merely as a delay due to response $\mathbf{A_{qu}^{f,1}}$.

Figure 5 plots the Nyquist diagram for the thermoacoustic loop for values of μ =0.01 (near non-reacting limit), 1.2, and 5. In the non-reacting limit, the thermoacoustic loop gain is zero and the noise to pressure response is characterized by acoustics alone (see Figure 3). With increasing μ, the increase in the loop gain - by factor μ - eventually causes the primary mode to become unstable for a critical value of $\mu \approx 1.2$ as shown in the Figure 5. Even for moderate values of μ, increased thermoacoustic loop gain and roll-off present in the heat release response can lead to eigenvalues close to imaginary axis causing large pressure oscillations due to noise excitation. Figure 6 compares the frequency response from noise (38) to pressure (at axial
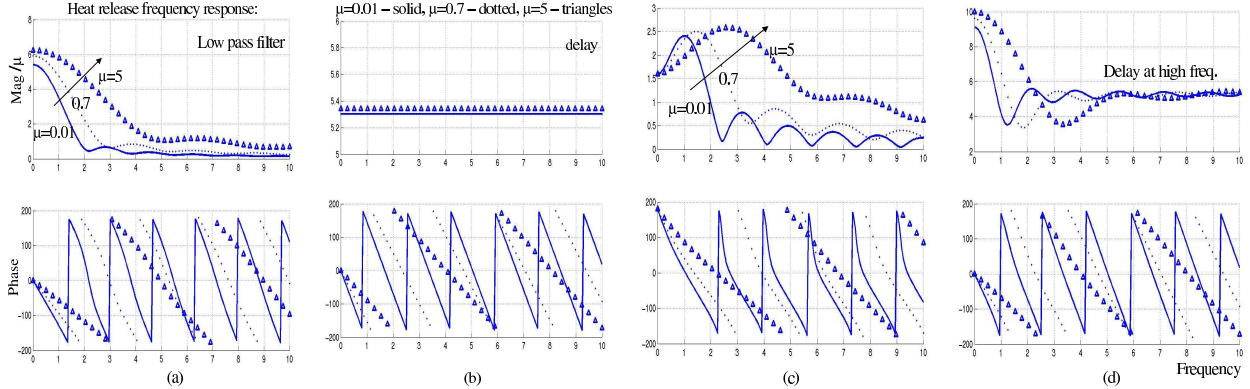
Fig. 4. Effect of density ratio on the frequency response for (a) $\mathbf{A_{qu}}(s)$, (b) $\mathbf{A_{qu}^{f,1}}(s)$, (c) $\mathbf{A_{qu}^{f,2}}(s)$, and (d) the cumulative $\mathbf{A_{qu}} + \mathbf{A_{qu}^{f,1}} + \mathbf{A_{qu}^{f,2}}(s)$ heat release transfer functions from acoustic velocity input ($\underline{u}^N(1) = 1$) to the heat release output $\underline{q}^N(1)$.
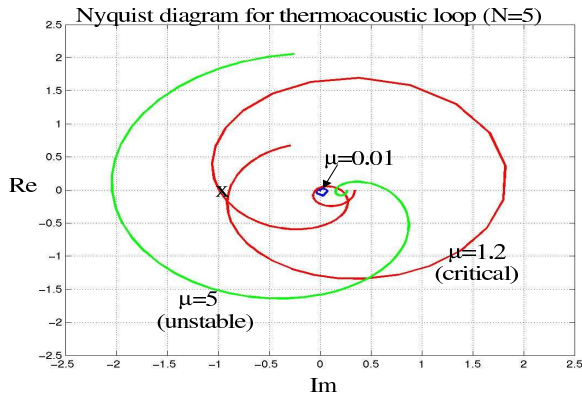

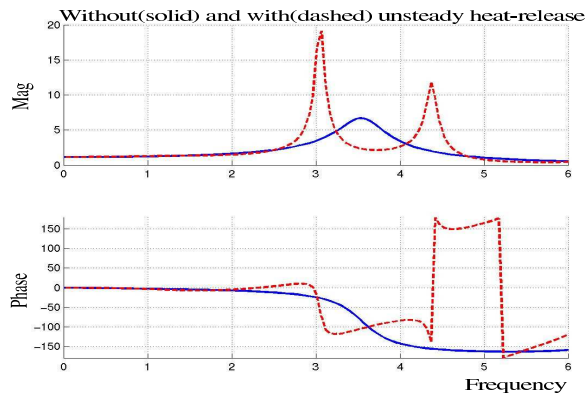Fig. 5. Effect of density ratio on the Nyquist diagram

Fig. 6. Effect of the unsteady heat release feedback on the frequency response from noise input (38) to the pressure sensor output evaluated at $x = 0$ ($\mu = 1$).

location $x = L_1$) with and with out unsteady heat release for a stable $\mu = 1$ case. The damped characteristics of acoustic submodel (because of mean heat release effects) together with delay induced roll-off present in the heat-release feedback leads to a *peaksplitting* in the response to noise for the coupled model as shown in the figure.

VII. CONCLUSIONS

In this paper, we studied the distributed linear dynamics of a coupled thermoacoustic problem. We showed that the density ratio parameter μ is very important in determining the magnitude and phase characteristics of both the acoustics (mean effects) and unsteady heat-release blocks. As the parameter μ increases, 1) the damping of the individual acoustic mode increases, 2) the acoustic modal frequency increases (due to increase in speed of sound), 3) the bandwidth of heat release response increases (physics of the problem becoming faster) and 4) the thermoacoustic loop gain increases. We also constructed a coupled thermoacoustic model that exhibits an instability as the density ratio parameter is increased beyond a critical value.

VIII. ACKNOWLEDGEMENTS

REFERENCES

[1] S. Candel, "Combustion dynamics and control: progress and challenges," *Procs. of Combustion Institute*, vol. 29, pp. 1–28, 2002.
[2] A. M. Annaswamy, M. Fleifil, J. P. Hathout, and A. Ghoniem, "Impact of linear coupling on the design of active controllers for thermoacoustic instability," *Combustion Science and Technology*, vol. 128, pp. 131–180, 1997.
[3] A. Dowling, "Nonlinear self-excited oscillations of a ducted flame," *Journal of Fluid Mechanics*, vol. 346, pp. 271–290, 1997.
[4] ——, "A kinematical model of ducted flame," *Journal of Fluid Mechanics*, vol. 394, pp. 51–72, 1999.
[5] P. G. Mehta, M. Soteriou, and A. Banaszuk, "Reduced order modelling of premixed flame dynamics in bluffbody combustors," *Submitted to Combustion and Flame*, 2003.
[6] M. Fleifil, A. Annaswamy, Z. Ghoniem, and A. Ghoniem, "Response of laminar premixed flame to flow oscillations: a kinematical model and thermoacoustic instability results," *Combustion and Flame*, vol. 106, pp. 487–510, 1996.
[7] S. Ducruix, D. Durox, and S. Candel, "Theoretical and experimental determination of the transfer function of a laminar premixed flame," *Proc. Combust. Inst.*, vol. 28, pp. 765–773, 2000.
[8] T. Schuller, D. Durox, and S. Candel, "A unified model for the prediction of laminar flame transfer functions: comparisons between conical and v-flame dynamics," *Combustion and Flame*, vol. 134, pp. 21–34, 2003.
[9] A. Banaszuk, G. Hagen, P. Mehta, and J. Oppelstrup, "A linear model for control of combustion instabilities on annular domain," *Procs. of IEEE CDC*, 2003.
[10] P. G. Mehta, A. Banaszuk, and M. Soteriou, "Fuel control of a ducted bluffbody flame," *Procs. of IEEE CDC*, 2003.